Supporting Information for

A Small Bimetallic Ag_3Cu_2 Nanocluster with Dual Emissions within and against Kasha's Rule

Rajini Anumula,[†,§] Pin Xiao,[‡,§] Chaonan Cui, [†] Haiming Wu,[†] Ganglong Cui,[‡,*] Wei-Hai Fang,[‡] Zhixun Luo,[†,*] and Jiannian Yao[†]

[†] State Key Laboratory for Structural Chemistry of Unstable and Stable Species, and Key Laboratory of Photochemistry, Institute of Chemistry, Chinese Academy of Sciences, Beijing 100090, China.

[‡] Key Laboratory of Theoretical and Computational Photochemistry, College of Chemistry, Beijing Normal University, Beijing 100875, China.

[*] Correspondence. Email: ganglong.cui@bnu.edu.cn (G.C.); zxluo@iccas.ac.cn (Z.L.)

[§] These authors contributed equally to this paper and share the first authorship.

Contents

S1. Experimental Methods

Chemicals. All reagents were of analytical grade and used without further purification. Also used, were silver nitrate ($AgNO_3$, Alfa Aesar, 98%), copper chloride ($CuCl_2$, Acros organics), 2, 4-dimethylbenzenethiol ($HSPhMe_2$, TCI 98%), sodium borohydride ($NaBH_4$, Acros 99.99%), tetraphenyl phosphonium bromide (PPh_4Br, Acros 99.99%). Distilled water was collected from Milli-Q (Millipore apparatus).

Characterization. Electrospray ionization time-of-flight mass spectrometry (ESI-TOF-MS) measurements were conducted by a MicroTOF-QIII High-resolution Mass Spectrometer in the negative ionization mode. The UV-Vis absorption spectra were collected using an UV-3600 Shimadzu UV-Vis-NIR Spectrophotometer. Photoluminescence spectra were recorded by a Horiba Scientific Fluoromax-4 spectrofluorometer.

Single crystal parsing. Single crystals of Ag_3Cu_2 clusters were grown for 4-5 days at -10 ºC by layering hexane over a concentrated DCM solution of clusters. The orange color crystals grown from the mixture were found to be suitable for X-ray diffraction. The diffraction data of $Ag_3Cu_2(SPhMe_2)_6$ were collected on an XtaLAB AFC10 (RCD3): fixed-chi single crystal X-ray diffractometer with Mo-Kα radiation (λ=0.71073 Å) at 173.15 K. Using Olex2, the structure was solved and refined using Full-matrix least-squares minimization based on F2 with structure solution program SHELXTL using Intrinsic Phasing with the SheLXTL refinement package. All non-hydrogen atoms were refined anisotropically, and all of the hydrogen atoms were set in geometrically calculated positions and refined isotropically using a riding model.

S2. TGA and XPS Patterns

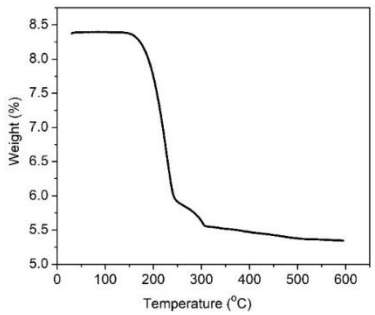

Fig. S1 The Thermogravimetric analysis of the Ag_3Cu_2 clusters.

The XPS spectrum of Ag 3d shows two peaks at binding energy values of 368.4 and 373.0 eV assigned to Ag $3d_{5/2}$ and Ag $3d_{3/2}$, suggesting the Ag valence state between Ag (0) and Ag (I). In the Cu 2p region, the spectrum shows two peaks at 932.3 and 952.0 eV, assigned to binding energy values of $2p_{3/2}$ and $2p_{1/2}$ electrons of Cu (0). No feature for Cu (II) electrons was observed, indicating the absence of Cu^{2+} in Ag_3Cu_2 clusters. That is, the valence state of the Cu atoms also lies in between 0 and +1 oxidation state. In addition, the binding energy of S $2p_{3/2}$ shows the peak at 162.0 eV which is characteristic of thiolates indicative of chemisorbed S species; the C 1s peak was located at 285.0 eV corresponding to unaffected characteristic of the ligand chain.

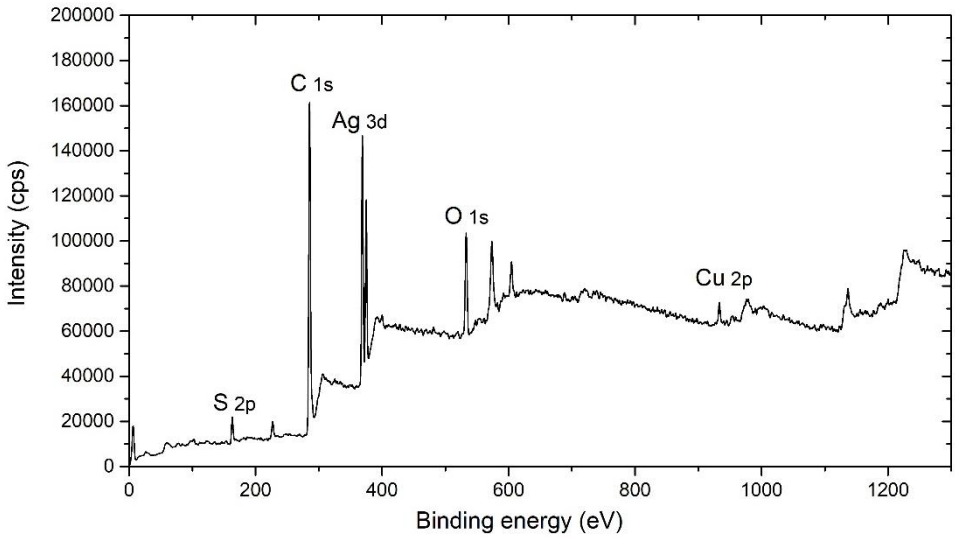

Fig. S2 The survey spectrum of XPS patterns of the Ag_3Cu_2 clusters.

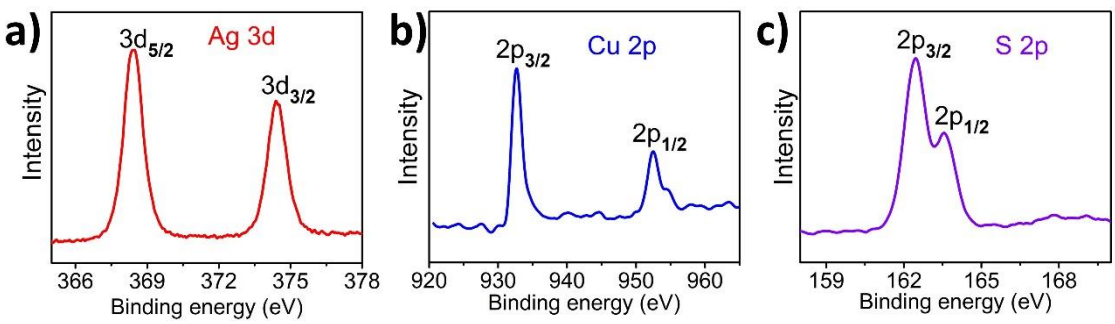

Fig. S3 XPS patterns of Ag 3d (a), S 2p (b) and Cu 2p (c) of the Ag_3Cu_2 clusters.

S3. Spectroscopic Characterization

Optical properties and luminescence mechanism of fluorescent nanomaterials are closely related to the development of optical technologies used in laser, lighting, and information display devices. Metal clusters bear discrete electronic states and exhibit molecule-like optical properties, allowing size-dependent fluorescence from ultraviolet-visible (UV-vis) to near-infrared (NIR) region. Despite predictable challenge in synthesizing very small bimetallic NCs, it is found that doping a hetero-atom into a small cluster could be much more sensitive to tune the property of nascent clusters. Among various approaches to synthesize fluorescent metal nanoclusters (NCs), a general issue lies in relatively low quantum yields of such metal NCs compared to fluorescent larger nanoparticles, quantum dots (QDs), and organic nanomaterials, which significantly limits practical applications of luminous metal NCs.

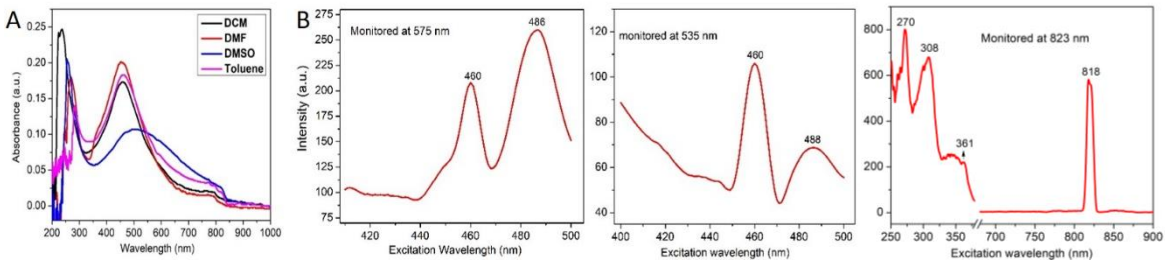

Fig. S4 (A) The UV-vis absorbance spectra of the Ag_3Cu_2 clusters in different solvents. **(B)** The fluorescence excitation spectra of $Ag_3Cu_2(SPhMe_2)_6$ clusters dissolved in DCM, monitored at 575nm, 535 nm and 823 nm respectively.

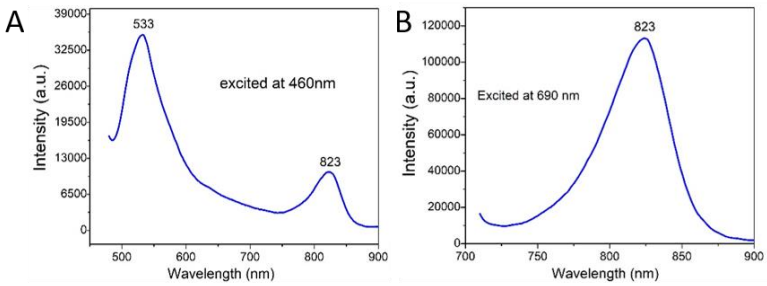

Fig. S5 Fluorescence emission spectra of $Ag_3Cu_2(SPhMe_2)_6$ clusters dissolved in DCM, excited at 460nm **(A)** and 690nm **(B)** respectively.

S4. Details of Single Crystal Data of $Ag_3Cu_2(SPhMe_2)_6$

Dark-orange block crystal of $C_{73}H_{76}Ag_3Cl_2Cu_2PS_6$, dimensions 0.289 × 0.163 × 0.156 mm^3, *Mr* = 1698.25, monoclinic, P 1 21/n 1, a = 14.5564(11) Å, b = 33.710(3) Å, c = 14.6416(11) Å, α = 90°, *β* = 94.2190(10)°, *γ* = 90°, *V* = 7165.2(9) Å3, *T* = 173.15 K, *Z* = 4, *Z'* = 1, *μ* (Mo Kα) = 3.508 mm-1, 56439 reflections measured, 16363 unique (*Rint* = 0.0365) which were used in all calculations. The final *wR2* was 0.1117 (all data) and *R1* was 0.0529 (I > 2(I)).

The Ag_3Cu_2 cluster is linked together by Ag–S-Cu, Cu–Ag, and Ag–Ag bonds. There is no bonding between the two Cu atoms indicating negligible Cu-Cu interactions in this cluster; in contrast, there is argentophilic interaction since the Ag1–Ag3 bond distance of 3.300 Å (cal. 3.331 Å) is shorter than the sum of the van der Waals radii of two Ag atoms (3.440 Å), pertaining to the weak $d_{10} – d_{10}$ interaction. The silver atoms are bound to the Cu1 atom with bond distances of 2.871-3.039 Å (cal. 2.862-2.991 Å) and Cu2 atom with 2.927-2.994 Å (cal. 2.874-2.967 Å) in a tetrahedral fashion. Comparing with previously published studies, most metal NCs (typically M_{25}, M=Au, Ag, Cu, etc.) favor an icosahedral 13-atom core structure, while a few others correspond to a metallic core of 12-atom cage, such as $Ag_{44}(SR)_{30}$ and Au_{32} NCs. Another interesting cluster, $Al_{50}Cp^*_{12}$ ($Cp^*=C_5Me_5$), bears an Al_8 center surrounded by 30 Al atoms to form 12 pentagonal faces that are capped by 12 Al-Cp^* moieties.

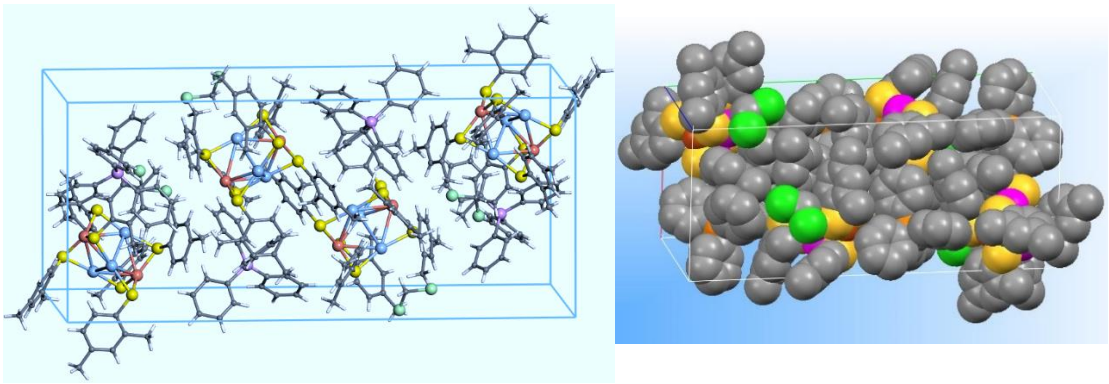

Fig. S6 The single-crystal packing structure of the Ag_3Cu_2 clusters. Color scheme: blue, silver; red, copper; yellow, sulfur; dark gray, carbon; purple, phosphorus; green, chlorine; white, hydrogen.

Table S1. Crystal data and structure refinement

Identification code	mx6667	
Empirical formula	C73 H76 Ag3 Cl2 Cu2 P S6	
Formula weight	1698.25	
Temperature	173.15 K	
Wavelength	0.71073 Å	
Crystal system	Monoclinic	
Space group	P 1 21/n 1	
Unit cell dimensions	a = 14.5564(11) Å	= 90°.
	b = 33.710(3) Å	= 94.2190(10)°
	c = 14.6416(11) Å	= 90°.
Volume	7165.2(9) $Å^3$	
Z	4	
Density (calculated)	1.574 Mg/m^3	
Absorption coefficient	1.702 mm^{-1}	
F(000)	3432	
Crystal size	0.289 x 0.163 x 0.156 mm^3	
Theta range for data collection	1.208 to 27.486°.	
Index ranges	-18<=h<=18, -43<=k<=43, -19<=l<=18	
Reflections collected	56439	
Independent reflections	16363 [R(int) = 0.0365]	
Completeness to theta = 25.242°	99.7 %	
Absorption correction	Semi-empirical from equivalents	
Max. and min. transmission	1.00000 and 0.87228	
Refinement method	Full-matrix least-squares on F^2	
Data / restraints / parameters	16363 / 0 / 796	
Goodness-of-fit on F^2	1.134	
Final R indices [I>2sigma(I)]	R1 = 0.0494, wR2 = 0.1095	
R indices (all data)	R1 = 0.0529, wR2 = 0.1117	
Extinction coefficient	n/a	
Largest diff. peak and hole	1.431 and -1.181 $e.Å^{-3}$	

Table S2. Atomic coordinates ($\times 10^4$) and equivalent isotropic displacement parameters ($Å^2 \cdot 10^3$) for $Ag_3Cu_2(SPhMe_2)_6$. U(eq) is defined as one third of the trace of the orthogonalized U^{ij} tensor.

	x	y	z	U(eq)
Ag1	8651(1)	3813(1)	6588(1)	43(1)
C1	9367(3)	3832(1)	8819(3)	34(1)
Cu1	7573(1)	4300(1)	7760(1)	31(1)
S1	9118(1)	4189(1)	7929(1)	39(1)
S2	6812(1)	4697(1)	6722(1)	40(1)
Ag2	6470(1)	4078(1)	5991(1)	44(1)
Cu2	7216(1)	3252(1)	5937(1)	27(1)
C2	10028(3)	3533(1)	8745(3)	40(1)
Ag3	7095(1)	3476(1)	7867(1)	44(1)
S3	8567(1)	3409(1)	5247(1)	37(1)
C3	10211(3)	3277(1)	9486(3)	45(1)
S4	5927(1)	3503(1)	5180(1)	37(1)
C4	9780(3)	3313(1)	10298(3)	47(1)
S5	7238(1)	2840(1)	7171(1)	36(1)
C5	9152(3)	3615(2)	10363(3)	48(1)
C6	8943(3)	3866(1)	9634(3)	41(1)
S6	6685(1)	4012(1)	8834(1)	38(1)
C7	10539(4)	3482(2)	7895(4)	65(2)
C8	9980(4)	3021(2)	11074(4)	70(2)
C9	7578(3)	4959(1)	6031(3)	38(1)
C10	7253(3)	5125(1)	5191(3)	42(1)
C11	7848(3)	5357(1)	4726(3)	49(1)
C12	8761(3)	5423(1)	5032(4)	51(1)
C13	9072(3)	5246(1)	5841(4)	55(1)
C14	8491(3)	5020(1)	6338(4)	50(1)
C15	6281(3)	5052(2)	4791(4)	57(1)

C16	9381(4)	5676(2)	4495(4)	70(2)
C17	8259(2)	3712(1)	4272(3)	31(1)
C18	8158(2)	3531(1)	3406(3)	32(1)
C19	7928(3)	3766(1)	2647(3)	38(1)
C20	7842(3)	4176(1)	2691(3)	42(1)
C21	7961(3)	4348(1)	3557(3)	42(1)
C22	8162(3)	4122(1)	4336(3)	37(1)
C23	8317(3)	3093(1)	3297(3)	45(1)
C24	7626(4)	4418(2)	1845(4)	65(2)
C25	4874(3)	3363(1)	5665(3)	33(1)
C26	4044(3)	3526(1)	5304(3)	39(1)
C27	3227(3)	3391(1)	5636(3)	45(1)
C28	3197(3)	3098(1)	6304(3)	42(1)
C29	4037(3)	2948(1)	6666(3)	41(1)
C30	4861(3)	3079(1)	6353(3)	36(1)
C31	4016(4)	3838(2)	4569(4)	57(1)
C32	2298(3)	2943(2)	6597(4)	61(1)
C33	8369(3)	2660(1)	7498(3)	32(1)
C34	8612(3)	2542(1)	8401(3)	37(1)
C35	9478(3)	2372(1)	8597(3)	41(1)
C36	10109(3)	2325(1)	7939(3)	40(1)
C37	9853(3)	2446(1)	7050(3)	43(1)
C38	8997(3)	2612(1)	6834(3)	40(1)
C39	7995(3)	2616(2)	9168(3)	51(1)
C40	11055(3)	2159(2)	8176(4)	55(1)
C41	5508(3)	4131(1)	8536(3)	32(1)
C42	5026(3)	4361(1)	9142(3)	33(1)
C43	4117(3)	4456(1)	8902(3)	37(1)
C44	3637(3)	4322(1)	8102(3)	41(1)
C45	4116(3)	4088(1)	7518(3)	44(1)
C46	5035(3)	3993(1)	7731(3)	40(1)
C47	5483(3)	4498(1)	10041(3)	46(1)

C48	2634(3)	4414(2)	7904(4)	59(1)
P1	2586(1)	3897(1)	1417(1)	28(1)
C49	1854(3)	3753(1)	2297(3)	34(1)
C50	2150(3)	3452(1)	2897(3)	42(1)
C51	1589(3)	3335(2)	3578(3)	50(1)
C52	752(3)	3522(2)	3665(3)	49(1)
C53	468(3)	3823(2)	3085(3)	49(1)
C54	1014(3)	3942(1)	2392(3)	40(1)
C55	2098(2)	4318(1)	801(2)	28(1)
C56	2483(3)	4696(1)	859(3)	32(1)
C57	2055(3)	5006(1)	375(3)	35(1)
C58	1246(3)	4943(1)	-163(3)	36(1)
C59	869(3)	4568(1)	-235(3)	36(1)
C60	1287(3)	4255(1)	244(3)	34(1)
C61	2686(3)	3509(1)	593(3)	31(1)
C62	3026(3)	3616(1)	-239(3)	41(1)
C63	3144(3)	3331(1)	-904(3)	47(1)
C64	2922(3)	2942(1)	-745(3)	47(1)
C65	2577(3)	2834(1)	73(3)	45(1)
C66	2462(3)	3114(1)	753(3)	37(1)
C67	3708(2)	4009(1)	1943(3)	31(1)
C68	4465(3)	3773(1)	1788(3)	42(1)
C69	5316(3)	3863(2)	2213(3)	51(1)
C70	5425(3)	4192(2)	2776(3)	47(1)
C71	4679(3)	4429(1)	2926(3)	41(1)
C72	3813(3)	4334(1)	2530(3)	35(1)
Cl1	4721(1)	7415(1)	540(2)	106(1)
Cl2	3610(2)	6845(1)	-564(1)	88(1)
C73	4399(5)	6929(3)	366(8)	153(5)

Table S3. Anisotropic displacement parameters ($Å^2 \cdot 10^3$) for $Ag_3Cu_2(SPhMe_2)_6$. The anisotropic displacement factor exponent takes the form: $-2^2 [h^2 a^{*2} U^{11} + ... + 2 h k a^* b^* U^{12}]$

	U^{11}	U^{22}	U^{33}	U^{23}	U^{13}	U^{12}
Ag1	42(1)	58(1)	29(1)	-1(1)	0(1)	-9(1)
C1	29(2)	34(2)	37(2)	-3(2)	-2(2)	-5(2)
Cu1	30(1)	29(1)	34(1)	-1(1)	1(1)	-1(1)
S1	40(1)	42(1)	35(1)	4(1)	-2(1)	-7(1)
S2	38(1)	31(1)	53(1)	-4(1)	6(1)	-3(1)
Ag2	46(1)	32(1)	53(1)	-5(1)	5(1)	-11(1)
Cu2	27(1)	27(1)	26(1)	-1(1)	3(1)	0(1)
C2	34(2)	41(2)	43(2)	-13(2)	-3(2)	1(2)
Ag3	45(1)	37(1)	51(1)	-8(1)	10(1)	7(1)
S3	33(1)	47(1)	31(1)	4(1)	4(1)	3(1)
C3	40(2)	30(2)	62(3)	-6(2)	-10(2)	6(2)
S4	43(1)	36(1)	33(1)	-2(1)	4(1)	-8(1)
C4	39(2)	43(2)	57(3)	11(2)	-6(2)	-9(2)
S5	32(1)	34(1)	42(1)	-4(1)	2(1)	3(1)
C5	42(2)	58(3)	44(2)	12(2)	7(2)	0(2)
C6	37(2)	45(2)	42(2)	4(2)	6(2)	6(2)
S6	39(1)	37(1)	39(1)	-5(1)	7(1)	2(1)
C7	51(3)	92(4)	51(3)	-23(3)	0(2)	21(3)
C8	70(4)	53(3)	86(4)	31(3)	-10(3)	-10(3)
C9	39(2)	28(2)	48(2)	-6(2)	3(2)	-5(2)
C10	38(2)	43(2)	46(2)	-9(2)	3(2)	-2(2)
C11	55(3)	50(3)	42(2)	-4(2)	5(2)	-7(2)
C12	51(3)	45(2)	58(3)	-3(2)	8(2)	-13(2)
C13	40(3)	46(3)	76(4)	2(2)	-1(2)	-11(2)
C14	46(3)	37(2)	64(3)	6(2)	-6(2)	-7(2)
C15	43(3)	73(3)	52(3)	1(3)	-7(2)	-6(2)

C16	66(4)	70(4)	75(4)	10(3)	13(3)	-21(3)
C17	24(2)	38(2)	32(2)	0(2)	3(1)	-3(1)
C18	23(2)	41(2)	34(2)	-3(2)	5(1)	-6(2)
C19	32(2)	54(2)	28(2)	-3(2)	3(2)	-7(2)
C20	32(2)	53(2)	41(2)	7(2)	6(2)	-4(2)
C21	38(2)	38(2)	50(2)	4(2)	6(2)	0(2)
C22	33(2)	40(2)	37(2)	-7(2)	4(2)	-1(2)
C23	43(2)	39(2)	52(3)	-13(2)	2(2)	-8(2)
C24	69(4)	75(4)	50(3)	25(3)	3(3)	-2(3)
C25	40(2)	29(2)	29(2)	-7(1)	3(2)	-6(2)
C26	47(2)	37(2)	33(2)	-3(2)	-1(2)	-1(2)
C27	40(2)	54(3)	39(2)	-8(2)	-3(2)	1(2)
C28	41(2)	48(2)	37(2)	-12(2)	7(2)	-6(2)
C29	47(2)	38(2)	38(2)	2(2)	7(2)	-6(2)
C30	35(2)	32(2)	42(2)	-2(2)	2(2)	-3(2)
C31	55(3)	63(3)	52(3)	18(2)	-4(2)	8(2)
C32	45(3)	87(4)	52(3)	-8(3)	13(2)	-11(3)
C33	30(2)	29(2)	37(2)	-1(2)	0(2)	-2(1)
C34	41(2)	29(2)	40(2)	2(2)	6(2)	-3(2)
C35	45(2)	37(2)	41(2)	9(2)	-2(2)	-2(2)
C36	34(2)	38(2)	49(2)	8(2)	-4(2)	-1(2)
C37	37(2)	51(2)	43(2)	2(2)	7(2)	8(2)
C38	39(2)	47(2)	34(2)	0(2)	1(2)	8(2)
C39	51(3)	63(3)	42(2)	8(2)	12(2)	4(2)
C40	42(3)	65(3)	56(3)	14(2)	-5(2)	6(2)
C41	39(2)	28(2)	32(2)	-4(1)	11(2)	-7(2)
C42	40(2)	29(2)	31(2)	-4(1)	6(2)	-4(2)
C43	42(2)	33(2)	37(2)	-6(2)	11(2)	1(2)
C44	43(2)	40(2)	40(2)	2(2)	8(2)	-2(2)
C45	43(2)	55(3)	33(2)	-9(2)	4(2)	-9(2)
C46	44(2)	41(2)	36(2)	-13(2)	8(2)	-5(2)
C47	46(2)	55(3)	36(2)	-16(2)	5(2)	3(2)

C48	45(3)	79(4)	51(3)	-4(3)	-2(2)	7(3)
P1	26(1)	26(1)	33(1)	0(1)	0(1)	0(1)
C49	29(2)	34(2)	37(2)	-1(2)	2(2)	-5(2)
C50	38(2)	50(2)	38(2)	6(2)	0(2)	-1(2)
C51	55(3)	54(3)	41(2)	11(2)	0(2)	-12(2)
C52	48(3)	59(3)	41(2)	-3(2)	11(2)	-19(2)
C53	35(2)	58(3)	54(3)	1(2)	11(2)	-5(2)
C54	33(2)	42(2)	45(2)	2(2)	4(2)	0(2)
C55	25(2)	26(2)	32(2)	-1(1)	2(1)	1(1)
C56	27(2)	30(2)	37(2)	-3(2)	-2(2)	-1(1)
C57	34(2)	27(2)	45(2)	1(2)	4(2)	-3(2)
C58	33(2)	33(2)	41(2)	6(2)	3(2)	8(2)
C59	29(2)	39(2)	39(2)	1(2)	-5(2)	1(2)
C60	32(2)	29(2)	41(2)	1(2)	-3(2)	-6(2)
C61	28(2)	28(2)	36(2)	0(2)	-2(2)	1(1)
C62	50(2)	29(2)	44(2)	-1(2)	12(2)	-4(2)
C63	57(3)	41(2)	43(2)	-4(2)	11(2)	2(2)
C64	60(3)	35(2)	45(2)	-9(2)	-4(2)	9(2)
C65	60(3)	25(2)	50(3)	-1(2)	-2(2)	-1(2)
C66	44(2)	29(2)	38(2)	3(2)	0(2)	0(2)
C67	26(2)	34(2)	32(2)	2(2)	-1(1)	1(1)
C68	34(2)	47(2)	45(2)	-6(2)	0(2)	5(2)
C69	28(2)	67(3)	57(3)	-6(2)	-2(2)	14(2)
C70	28(2)	69(3)	43(2)	0(2)	-5(2)	-3(2)
C71	37(2)	46(2)	39(2)	-4(2)	-4(2)	-4(2)
C72	33(2)	38(2)	33(2)	-1(2)	-2(2)	2(2)
Cl1	81(1)	105(2)	132(2)	-39(1)	6(1)	11(1)
Cl2	111(1)	74(1)	82(1)	-10(1)	37(1)	-22(1)
C73	59(4)	136(8)	264(13)	143(9)	22(6)	7(5)

Table S4. Bond lengths [Å] for $Ag_3Cu_2(SPhMe_2)_6$.

Ag1-Cu1	2.9156(6)
Ag1-S1	2.3925(11)
Ag1-Ag2	3.3519(6)
Ag1-Cu2	2.9269(6)
Ag1-Ag3	3.2490(5)
Ag1-S3	2.3860(11)
C1-S1	1.790(4)
C1-C2	1.403(6)
C1-C6	1.388(6)
Cu1-S1	2.2752(12)
Cu1-S2	2.2553(12)
Cu1-Ag2	3.0390(6)
Cu1-Ag3	2.8711(6)
Cu1-S6	2.3209(12)
S2-Ag2	2.3800(11)
S2-C9	1.793(4)
Ag2-Cu2	2.9944(6)
Ag2-S4	2.3791(10)
Cu2-Ag3	2.9423(6)
Cu2-S3	2.3381(11)
Cu2-S4	2.2715(12)
Cu2-S5	2.2758(11)
C2-C3	1.397(6)
C2-C7	1.505(7)
Ag3-S5	2.3874(10)
Ag3-S6	2.3979(10)
S3-C17	1.786(4)
C3-H3	0.9500
C3-C4	1.390(7)
S4-C25	1.799(4)

C4-C5	1.375(7)
C4-C8	1.515(7)
S5-C33	1.787(4)
C5-H5	0.9500
C5-C6	1.380(6)
C6-H6	0.9500
S6-C41	1.783(4)
C7-H7A	0.9800
C7-H7B	0.9800
C7-H7C	0.9800
C8-H8A	0.9800
C8-H8B	0.9800
C8-H8C	0.9800
C9-C10	1.401(6)
C9-C14	1.386(6)
C10-C11	1.383(6)
C10-C15	1.511(6)
C11-H11	0.9500
C11-C12	1.389(7)
C12-C13	1.372(7)
C12-C16	1.505(7)
C13-H13	0.9500
C13-C14	1.384(7)
C14-H14	0.9500
C15-H15A	0.9800
C15-H15B	0.9800
C15-H15C	0.9800
C16-H16A	0.9800
C16-H16B	0.9800
C16-H16C	0.9800
C17-C18	1.406(5)
C17-C22	1.392(5)

C18-C19	1.385(6)
C18-C23	1.505(6)
C19-H19	0.9500
C19-C20	1.393(6)
C20-C21	1.392(6)
C20-C24	1.496(6)
C21-H21	0.9500
C21-C22	1.385(6)
C22-H22	0.9500
C23-H23A	0.9800
C23-H23B	0.9800
C23-H23C	0.9800
C24-H24A	0.9800
C24-H24B	0.9800
C24-H24C	0.9800
C25-C26	1.396(6)
C25-C30	1.391(6)
C26-C27	1.394(6)
C26-C31	1.504(6)
C27-H27	0.9500
C27-C28	1.393(7)
C28-C29	1.391(6)
C28-C32	1.500(6)
C29-H29	0.9500
C29-C30	1.388(6)
C30-H30	0.9500
C31-H31A	0.9800
C31-H31B	0.9800
C31-H31C	0.9800
C32-H32A	0.9800
C32-H32B	0.9800
C32-H32C	0.9800

C33-C34	1.400(6)
C33-C38	1.393(6)
C34-C35	1.396(6)
C34-C39	1.509(6)
C35-H35	0.9500
C35-C36	1.388(6)
C36-C37	1.389(6)
C36-C40	1.504(6)
C37-H37	0.9500
C37-C38	1.381(6)
C38-H38	0.9500
C39-H39A	0.9800
C39-H39B	0.9800
C39-H39C	0.9800
C40-H40A	0.9800
C40-H40B	0.9800
C40-H40C	0.9800
C41-C42	1.403(5)
C41-C46	1.400(6)
C42-C43	1.382(6)
C42-C47	1.503(5)
C43-H43	0.9500
C43-C44	1.394(6)
C44-C45	1.388(6)
C44-C48	1.501(6)
C45-H45	0.9500
C45-C46	1.388(6)
C46-H46	0.9500
C47-H47A	0.9800
C47-H47B	0.9800
C47-H47C	0.9800
C48-H48A	0.9800

C48-H48B	0.9800
C48-H48C	0.9800
P1-C49	1.798(4)
P1-C55	1.799(4)
P1-C61	1.793(4)
P1-C67	1.794(4)
C49-C50	1.390(6)
C49-C54	1.394(6)
C50-H50	0.9500
C50-C51	1.391(6)
C51-H51	0.9500
C51-C52	1.385(7)
C52-H52	0.9500
C52-C53	1.367(7)
C53-H53	0.9500
C53-C54	1.392(6)
C54-H54	0.9500
C55-C56	1.393(5)
C55-C60	1.401(5)
C56-H56	0.9500
C56-C57	1.382(5)
C57-H57	0.9500
C57-C58	1.384(6)
C58-H58	0.9500
C58-C59	1.379(6)
C59-H59	0.9500
C59-C60	1.384(5)
C60-H60	0.9500
C61-C62	1.396(6)
C61-C66	1.395(5)
C62-H62	0.9500
C62-C63	1.387(6)

C63-H63	0.9500
C63-C64	1.374(6)
C64-H64	0.9500
C64-C65	1.381(7)
C65-H65	0.9500
C65-C66	1.391(6)
C66-H66	0.9500
C67-C68	1.392(5)
C67-C72	1.395(5)
C68-H68	0.9500
C68-C69	1.378(6)
C69-H69	0.9500
C69-C70	1.385(7)
C70-H70	0.9500
C70-C71	1.379(6)
C71-H71	0.9500
C71-C72	1.384(6)
C72-H72	0.9500
Cl1-C73	1.718(10)
Cl2-C73	1.739(11)
C73-H73A	0.9900
C73-H73B	0.9900

Table S5. Bond angles [°] for $Ag_3Cu_2(SPhMe_2)_6$.

Cu1-Ag1-Ag2	57.505(13)
Cu1-Ag1-Cu2	98.821(17)
Cu1-Ag1-Ag3	55.196(13)
S1-Ag1-Cu1	49.57(3)
S1-Ag1-Ag2	106.21(3)
S1-Ag1-Cu2	139.66(3)
S1-Ag1-Ag3	83.11(3)
Cu2-Ag1-Ag2	56.479(12)
Cu2-Ag1-Ag3	56.613(13)
Ag3-Ag1-Ag2	63.664(12)
S3-Ag1-Cu1	143.99(3)
S3-Ag1-S1	166.42(4)
S3-Ag1-Ag2	86.99(3)
S3-Ag1-Cu2	50.98(3)
S3-Ag1-Ag3	106.18(3)
C2-C1-S1	122.0(3)
C6-C1-S1	119.5(3)
C6-C1-C2	118.4(4)
Ag1-Cu1-Ag2	68.479(14)
S1-Cu1-Ag1	53.17(3)
S1-Cu1-Ag2	120.52(3)
S1-Cu1-Ag3	94.36(3)
S1-Cu1-S6	116.92(4)
S2-Cu1-Ag1	101.31(3)
S2-Cu1-S1	127.15(4)
S2-Cu1-Ag2	50.83(3)
S2-Cu1-Ag3	120.13(3)
S2-Cu1-S6	115.78(4)
Ag3-Cu1-Ag1	68.309(14)
Ag3-Cu1-Ag2	72.146(14)
S6-Cu1-Ag1	120.93(3)

S6-Cu1-Ag2	100.89(3)
S6-Cu1-Ag3	53.75(3)
C1-S1-Ag1	105.81(13)
C1-S1-Cu1	109.60(13)
Cu1-S1-Ag1	77.26(3)
Cu1-S2-Ag2	81.89(4)
C9-S2-Cu1	112.16(15)
C9-S2-Ag2	107.21(14)
Cu1-Ag2-Ag1	54.016(12)
S2-Ag2-Ag1	87.37(3)
S2-Ag2-Cu1	47.28(3)
S2-Ag2-Cu2	139.78(3)
Cu2-Ag2-Ag1	54.577(12)
Cu2-Ag2-Cu1	94.672(16)
S4-Ag2-Ag1	100.73(3)
S4-Ag2-Cu1	139.58(3)
S4-Ag2-S2	171.79(4)
S4-Ag2-Cu2	48.36(3)
Ag1-Cu2-Ag2	68.944(14)
Ag1-Cu2-Ag3	67.225(13)
Ag3-Cu2-Ag2	71.831(14)
S3-Cu2-Ag1	52.46(3)
S3-Cu2-Ag2	96.79(3)
S3-Cu2-Ag3	117.94(3)
S4-Cu2-Ag1	117.49(3)
S4-Cu2-Ag2	51.51(3)
S4-Cu2-Ag3	105.51(3)
S4-Cu2-S3	113.26(4)
S4-Cu2-S5	125.30(4)
S5-Cu2-Ag1	99.65(3)
S5-Cu2-Ag2	122.01(3)
S5-Cu2-Ag3	52.59(3)

S5-Cu2-S3	121.23(4)
C1-C2-C7	121.9(4)
C3-C2-C1	118.5(4)
C3-C2-C7	119.6(4)
Cu1-Ag3-Ag1	56.494(13)
Cu1-Ag3-Cu2	99.486(17)
Cu2-Ag3-Ag1	56.162(12)
S5-Ag3-Ag1	88.98(3)
S5-Ag3-Cu1	144.70(3)
S5-Ag3-Cu2	49.21(3)
S5-Ag3-S6	163.96(4)
S6-Ag3-Ag1	106.93(3)
S6-Ag3-Cu1	51.31(3)
S6-Ag3-Cu2	142.74(3)
Cu2-S3-Ag1	76.56(3)
C17-S3-Ag1	108.96(13)
C17-S3-Cu2	107.77(12)
C2-C3-H3	118.7
C4-C3-C2	122.5(4)
C4-C3-H3	118.7
Cu2-S4-Ag2	80.12(4)
C25-S4-Ag2	106.17(12)
C25-S4-Cu2	113.94(14)
C3-C4-C8	120.7(5)
C5-C4-C3	117.9(4)
C5-C4-C8	121.3(5)
Cu2-S5-Ag3	78.20(3)
C33-S5-Cu2	112.25(13)
C33-S5-Ag3	107.34(13)
C4-C5-H5	119.7
C4-C5-C6	120.7(4)
C6-C5-H5	119.7

C1-C6-H6	119.0
C5-C6-C1	121.9(4)
C5-C6-H6	119.0
Cu1-S6-Ag3	74.93(3)
C41-S6-Cu1	108.22(13)
C41-S6-Ag3	107.57(13)
C2-C7-H7A	109.5
C2-C7-H7B	109.5
C2-C7-H7C	109.5
H7A-C7-H7B	109.5
H7A-C7-H7C	109.5
H7B-C7-H7C	109.5
C4-C8-H8A	109.5
C4-C8-H8B	109.5
C4-C8-H8C	109.5
H8A-C8-H8B	109.5
H8A-C8-H8C	109.5
H8B-C8-H8C	109.5
C10-C9-S2	120.5(3)
C14-C9-S2	120.8(4)
C14-C9-C10	118.6(4)
C9-C10-C15	121.5(4)
C11-C10-C9	118.3(4)
C11-C10-C15	120.2(4)
C10-C11-H11	118.3
C10-C11-C12	123.4(5)
C12-C11-H11	118.3
C11-C12-C16	121.2(5)
C13-C12-C11	117.2(4)
C13-C12-C16	121.7(5)
C12-C13-H13	119.4
C12-C13-C14	121.1(5)

C14-C13-H13	119.4
C9-C14-H14	119.3
C13-C14-C9	121.3(5)
C13-C14-H14	119.3
C10-C15-H15A	109.5
C10-C15-H15B	109.5
C10-C15-H15C	109.5
H15A-C15-H15B	109.5
H15A-C15-H15C	109.5
H15B-C15-H15C	109.5
C12-C16-H16A	109.5
C12-C16-H16B	109.5
C12-C16-H16C	109.5
H16A-C16-H16B	109.5
H16A-C16-H16C	109.5
H16B-C16-H16C	109.5
C18-C17-S3	118.3(3)
C22-C17-S3	122.3(3)
C22-C17-C18	119.3(4)
C17-C18-C23	121.1(4)
C19-C18-C17	118.5(4)
C19-C18-C23	120.3(4)
C18-C19-H19	118.4
C18-C19-C20	123.2(4)
C20-C19-H19	118.4
C19-C20-C24	121.1(4)
C21-C20-C19	116.7(4)
C21-C20-C24	122.2(5)
C20-C21-H21	119.1
C22-C21-C20	121.8(4)
C22-C21-H21	119.1
C17-C22-H22	119.8

C21-C22-C17	120.4(4)
C21-C22-H22	119.8
C18-C23-H23A	109.5
C18-C23-H23B	109.5
C18-C23-H23C	109.5
H23A-C23-H23B	109.5
H23A-C23-H23C	109.5
H23B-C23-H23C	109.5
C20-C24-H24A	109.5
C20-C24-H24B	109.5
C20-C24-H24C	109.5
H24A-C24-H24B	109.5
H24A-C24-H24C	109.5
H24B-C24-H24C	109.5
C26-C25-S4	119.1(3)
C30-C25-S4	121.6(3)
C30-C25-C26	119.2(4)
C25-C26-C31	121.6(4)
C27-C26-C25	118.5(4)
C27-C26-C31	119.9(4)
C26-C27-H27	118.4
C28-C27-C26	123.2(4)
C28-C27-H27	118.4
C27-C28-C32	121.3(4)
C29-C28-C27	117.0(4)
C29-C28-C32	121.7(4)
C28-C29-H29	119.5
C30-C29-C28	121.0(4)
C30-C29-H29	119.5
C25-C30-H30	119.5
C29-C30-C25	121.1(4)
C29-C30-H30	119.5

C26-C31-H31A	109.5
C26-C31-H31B	109.5
C26-C31-H31C	109.5
H31A-C31-H31B	109.5
H31A-C31-H31C	109.5
H31B-C31-H31C	109.5
C28-C32-H32A	109.5
C28-C32-H32B	109.5
C28-C32-H32C	109.5
H32A-C32-H32B	109.5
H32A-C32-H32C	109.5
H32B-C32-H32C	109.5
C34-C33-S5	120.9(3)
C38-C33-S5	119.4(3)
C38-C33-C34	119.6(4)
C33-C34-C39	122.2(4)
C35-C34-C33	118.2(4)
C35-C34-C39	119.5(4)
C34-C35-H35	118.8
C36-C35-C34	122.5(4)
C36-C35-H35	118.8
C35-C36-C37	118.2(4)
C35-C36-C40	121.6(4)
C37-C36-C40	120.2(4)
C36-C37-H37	119.7
C38-C37-C36	120.6(4)
C38-C37-H37	119.7
C33-C38-H38	119.5
C37-C38-C33	121.0(4)
C37-C38-H38	119.5
C34-C39-H39A	109.5
C34-C39-H39B	109.5

C34-C39-H39C	109.5
H39A-C39-H39B	109.5
H39A-C39-H39C	109.5
H39B-C39-H39C	109.5
C36-C40-H40A	109.5
C36-C40-H40B	109.5
C36-C40-H40C	109.5
H40A-C40-H40B	109.5
H40A-C40-H40C	109.5
H40B-C40-H40C	109.5
C42-C41-S6	119.1(3)
C46-C41-S6	122.4(3)
C46-C41-C42	118.5(4)
C41-C42-C47	120.9(4)
C43-C42-C41	118.8(4)
C43-C42-C47	120.3(4)
C42-C43-H43	118.3
C42-C43-C44	123.3(4)
C44-C43-H43	118.3
C43-C44-C48	121.0(4)
C45-C44-C43	117.2(4)
C45-C44-C48	121.7(4)
C44-C45-H45	119.6
C46-C45-C44	120.8(4)
C46-C45-H45	119.6
C41-C46-H46	119.4
C45-C46-C41	121.3(4)
C45-C46-H46	119.4
C42-C47-H47A	109.5
C42-C47-H47B	109.5
C42-C47-H47C	109.5
H47A-C47-H47B	109.5

H47A-C47-H47C	109.5
H47B-C47-H47C	109.5
C44-C48-H48A	109.5
C44-C48-H48B	109.5
C44-C48-H48C	109.5
H48A-C48-H48B	109.5
H48A-C48-H48C	109.5
H48B-C48-H48C	109.5
C49-P1-C55	109.85(18)
C61-P1-C49	111.51(18)
C61-P1-C55	106.69(17)
C61-P1-C67	108.98(18)
C67-P1-C49	108.56(18)
C67-P1-C55	111.26(17)
C50-C49-P1	118.5(3)
C50-C49-C54	120.2(4)
C54-C49-P1	121.3(3)
C49-C50-H50	120.4
C49-C50-C51	119.2(4)
C51-C50-H50	120.4
C50-C51-H51	119.8
C52-C51-C50	120.3(4)
C52-C51-H51	119.8
C51-C52-H52	119.7
C53-C52-C51	120.5(4)
C53-C52-H52	119.7
C52-C53-H53	119.9
C52-C53-C54	120.2(4)
C54-C53-H53	119.9
C49-C54-H54	120.2
C53-C54-C49	119.6(4)
C53-C54-H54	120.2

C56-C55-P1	123.3(3)
C56-C55-C60	119.5(3)
C60-C55-P1	117.1(3)
C55-C56-H56	120.1
C57-C56-C55	119.7(3)
C57-C56-H56	120.1
C56-C57-H57	119.7
C56-C57-C58	120.6(4)
C58-C57-H57	119.7
C57-C58-H58	120.0
C59-C58-C57	120.0(4)
C59-C58-H58	120.0
C58-C59-H59	119.9
C58-C59-C60	120.3(4)
C60-C59-H59	119.9
C55-C60-H60	120.1
C59-C60-C55	119.9(3)
C59-C60-H60	120.1
C62-C61-P1	116.8(3)
C66-C61-P1	123.5(3)
C66-C61-C62	119.7(4)
C61-C62-H62	119.8
C63-C62-C61	120.3(4)
C63-C62-H62	119.8
C62-C63-H63	120.1
C64-C63-C62	119.9(4)
C64-C63-H63	120.1
C63-C64-H64	119.9
C63-C64-C65	120.2(4)
C65-C64-H64	119.9
C64-C65-H65	119.6
C64-C65-C66	120.8(4)

C66-C65-H65	119.6
C61-C66-H66	120.5
C65-C66-C61	119.0(4)
C65-C66-H66	120.5
C68-C67-P1	121.1(3)
C68-C67-C72	119.9(4)
C72-C67-P1	119.0(3)
C67-C68-H68	120.1
C69-C68-C67	119.8(4)
C69-C68-H68	120.1
C68-C69-H69	119.8
C68-C69-C70	120.4(4)
C70-C69-H69	119.8
C69-C70-H70	120.0
C71-C70-C69	120.1(4)
C71-C70-H70	120.0
C70-C71-H71	119.9
C70-C71-C72	120.3(4)
C72-C71-H71	119.9
C67-C72-H72	120.2
C71-C72-C67	119.6(4)
C71-C72-H72	120.2
Cl1-C73-Cl2	115.4(4)
Cl1-C73-H73A	108.4
Cl1-C73-H73B	108.4
Cl2-C73-H73A	108.4
Cl2-C73-H73B	108.4
H73A-C73-H73B	107.5

Symmetry transformations used to generate equivalent atoms.

S5. DFT and TDDFT Calculations

All density functional theory (DFT) and time-dependent density functional theory (TD-DFT) calculations were carried out using Gaussian09.

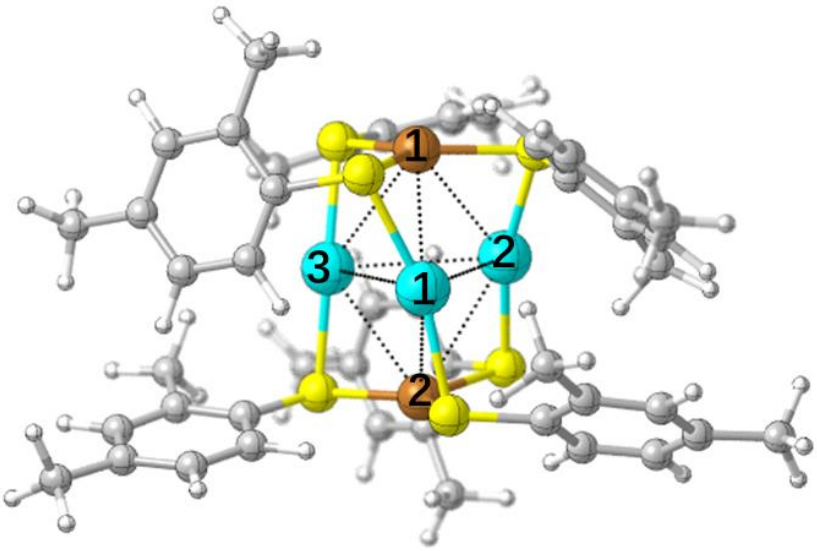

Fig. S7 The numbering of Ag_3Cu_2 in $[Ag_3Cu_2(SPhMe_2)_6]^-$ at the BP86 optimized S_0 minimum.

Table S6. DFT computed bond lengths (B.L. in Å) and Mayer bond orders (B.O.) of selected bonds in $[Ag_3Cu_2(SPhMe_2)_6]^-$ at the S_0 minimum.

Bonds	Ag1-Ag2	Ag2-Ag3	Ag3-Ag1	Ag1-Cu2	Ag2-Cu2	Ag3-Cu2	Ag1-Cu1
B.L.	3.312	3.421	3.261	2.874	2.967	2.881	2.862
B.O.	0.14	0.09	0.19	0.09	0.05	0.11	0.13
Bonds	Ag2-Cu1	Ag3-Cu1	Ag1-S	Ag2-S	Ag3-S	Cu1-S	Cu2-S
B.L.	2.991	2.907	2.438	2.432	2.436	2.325	2.325
B.O.	0.06	0.07	0.47	0.38	0.45	0.65	0.66

Table S7. DFT computed natural population analysis (NPA) charges of several key atoms in $[Ag_3Cu_2(SPhMe_2)_6]^-$ at the S_0 minimum.

Atoms	Ag1	Ag2	Ag3	Cu1	Cu2	S (avg)
NPA	0.29	0.33	0.30	0.05	0.05	-0.22

Table S8. TD-DFT computed wavelengths (nm, kcal/mol in brackets), oscillator strengths, and weights of electronic configurations (in %) of strong electronic excitation transitions at the optimized S_0 minimum of $[Ag_3Cu_2(SPhMe_2)_6]^-$.

state	wavelength	oscillator strength	electronic configuration
S_4	483 (59.2)	0.0673	HOMO-3 → LUMO (93)
S_6	457 (62.6)	0.0654	HOMO-5 → LUMO (94)
S_{11}	388 (73.7)	0.0245	HOMO-1 → LUMO+1 (72)
S_{88}	320 (89.3)	0.0429	HOMO-3 → LUMO+10 (37)
S_{226}	267 (107.1)	0.0224	HOMO-2 → LUMO+19 (26)

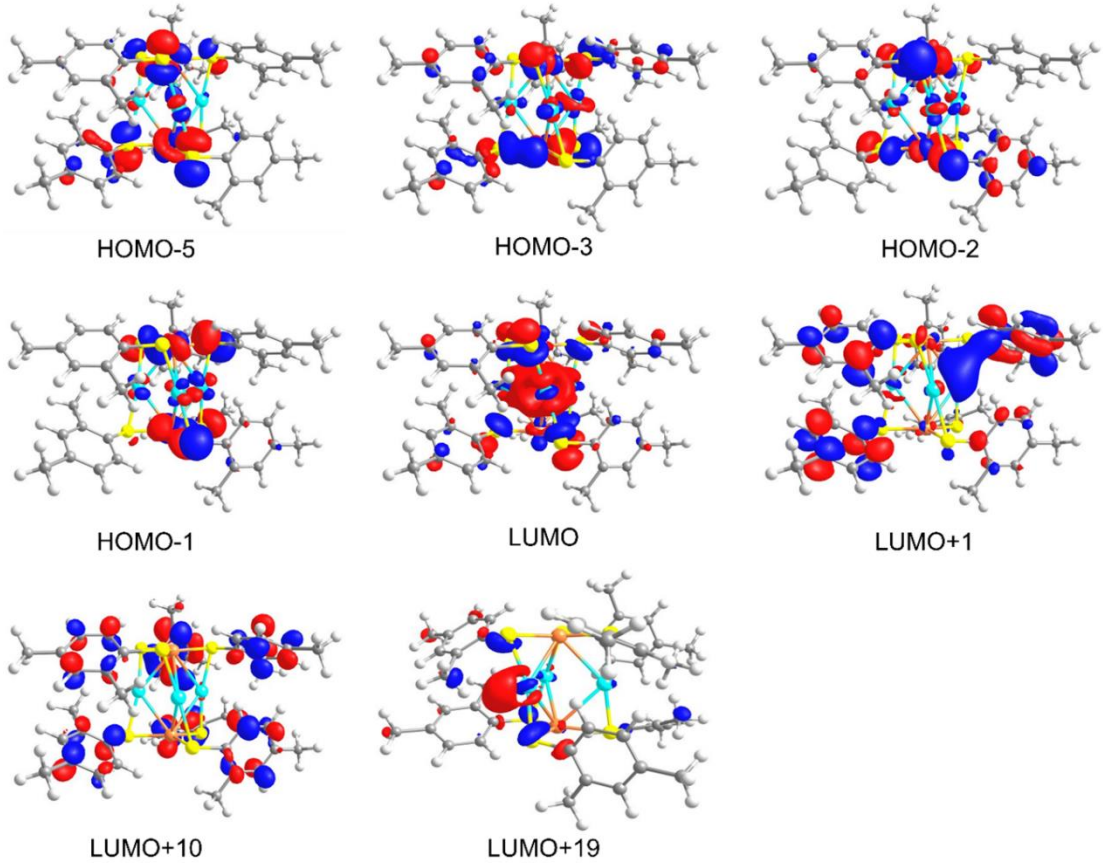

Fig. S8 TD-DFT calculated frontier molecular orbitals of $[Ag_3Cu_2(SPhMe_2)_6]^-$ at the S_0 minimum.

Table S9. TD-DFT computed wavelengths (nm, kcal/mol in brackets), oscillator strengths, and weights of electronic configurations (in %) of strong electronic de-excitation transitions at the optimized S_1 minimum of $[Ag_3Cu_2(SPhMe_2)_6]^-$.

state	wavelength	oscillator Strength	electronic configuration
S1	**833 (34.3)**	0.0083	LUMO → HOMO (99)
S2	642 (44.5)	0.0053	LUMO → HOMO-1 (97)
S3	**620 (46.1)**	0.0412	LUMO → HOMO-2 (93)
S4	608 (47.0)	0.0278	LUMO → HOMO-3 (95)
S5	**563 (50.8)**	0.0572	LUMO → HOMO-4 (97)
S6	550 (52.0)	0.0140	LUMO → HOMO-5 (96)
S7	**518 (55.2)**	0.0321	LUMO → HOMO-6 (83)

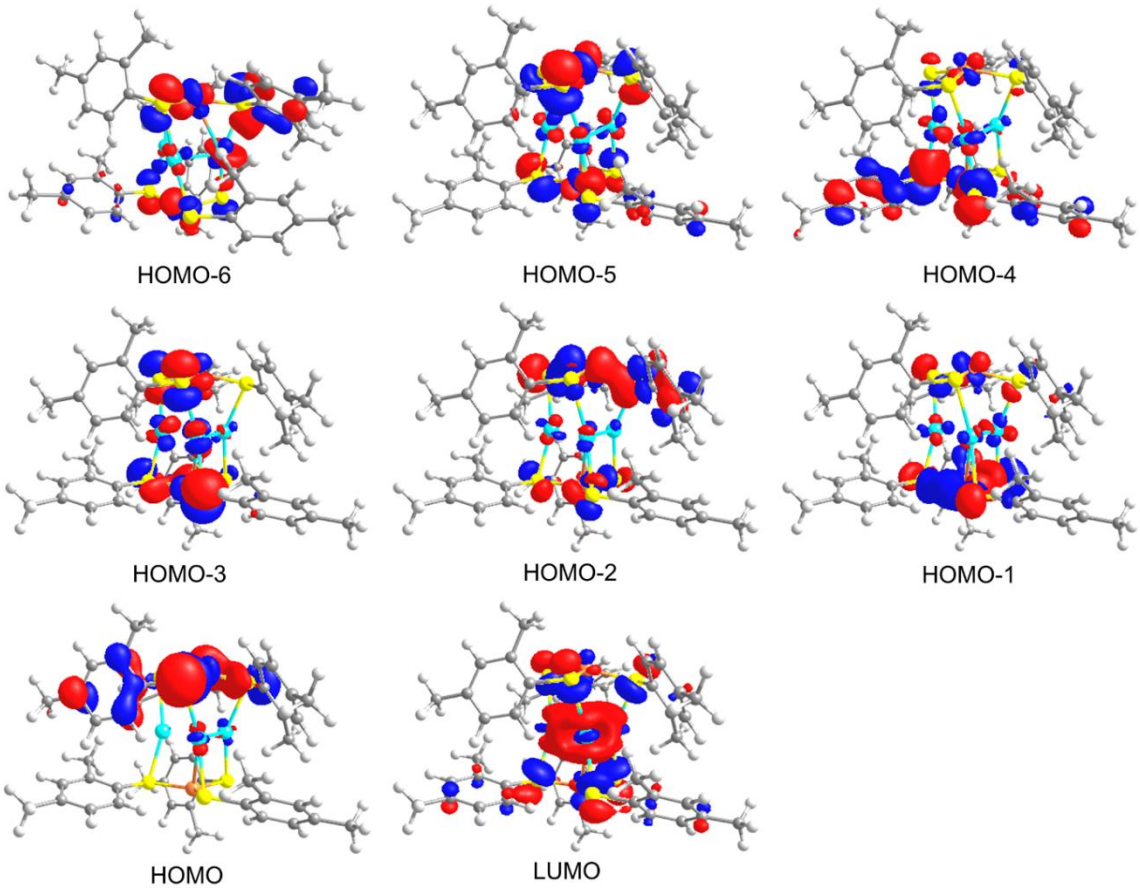

Fig. S9 TD-DFT calculated frontier molecular orbitals of $[Ag_3Cu_2(SPhMe_2)_6]^-$ at the S_1 minimum.

Table S10. TD-DFT calculated molecular orbital levels (in eV) and relevant weights (in %) with respect to Ag_3, Cu_2, and S, C, and H atoms of $[Ag_3Cu_2(SPhMe_2)_6]^-$ at its S_1 minimum.

Orbitals	E (in eV)	Weights (%)		
		Ag_3 (5sp+4d)	**Cu_2 (4sp+3d)**	**S, C, and H (S+CH)**
LUMO	-2.04	36.7 (29.7+7.0)	8.6 (4.5+4.1)	54.6 (36.4+18.2)
HOMO	-3.48	2.6 (1.1+1.5)	39.2 (1.7+37.5)	58.2 (41.3+16.9)
HOMO-1	-3.91	6.3 (2.2+4.1)	34.4 (1.5+32.9)	59.3 (40.8+18.5)
HOMO-2	-3.97	3.8 (1.4+2.4)	40.3 (0.7+39.6)	55.9 (38.5+17.4)
HOMO-3	-4.02	7.7 (0.7+7.0)	35.3 (0.8+34.6)	57.0 (45.3+11.7)
HOMO-4	-4.12	5.7 (1.8+3.9)	31.9 (0.6+31.3)	62.4 (38.7+23.7)
HOMO-5	-4.23	4.7 (0.2+4.5)	46.0 (1.1+44.9)	49.3 (38.6+10.7)
HOMO-6	-4.36	10.8 (5.8+5.0)	43.2 (1.0+42.2)	76.0 (62.7+13.3)

Table S11. TD-DFT computed vertical $T_1 \rightarrow S_0$ emission wavelength (nm, kcal/mol in bracket) and main electronic configuration at the T_1 minimum of $[Ag_3Cu_2(SPhMe_2)_6]^-$.

state	wavelength	oscillator Strength	electronic configuration
T_1	**975 (29.3)**	0	LUMO $\rightarrow$ HOMO (100)